Dalton
www.rsc.org/dalton

Synthesis and third-order nonlinear optical properties of $[Mo_3(\mu_3\text{-}S)(\mu_2\text{-}S_2)_3]^{4+}$ clusters with maleonitriledithiolate, oxalate and thiocyanate ligands

Juan Manuel Garriga,[a] Rosa Llusar,*[a] Santiago Uriel,[b] Cristian Vicent,[a] Alistair J. Usher,[c] Nigel T. Lucas,[c] Mark G. Humphrey[c] and Marek Samoc[d]

[a] *Departament de Ciències Experimentals, Universitat Jaume I Campus de Riu Sec, Box 224, Castelló, Spain. E-mail: llusar@exp.uji.es*

[b] *Departamento de Química Orgánica-Química Física, Centro Politécnico Superior, Universidad de Zaragoza, María de Luna 3, 50015, Zaragoza, Spain. E-mail: suriel@posta.unizar.es*

[c] *Department of Chemistry, Australian National University, Canberra, ACT 0200, Australia. E-mail: Mark.Humphrey@anu.edu.au*

[d] *Australian Photonics Cooperative Research Centre, Laser Physics Centre, Research School of Physical Sciences and Engineering, Australian National University, Canberra, ACT 0200, Australia. E-mail: mjs111@rsphy1.anu.edu.au*

Received 8th July 2003, Accepted 19th September 2003
First published as an Advance Article on the web 30th September 2003

Substitution of the bromine ligands in $[(n\text{-}Bu)_4N]_2[Mo_3S_7Br_6]$ (**1**) by bidentate ligands such as maleonitriledithiolate (mnt) or oxalate (ox) affords the trinuclear clusters $[Mo_3S_7(mnt)_3]^{2-}$ ($[\mathbf{2}]^{2-}$) and $[Mo_3S_7(ox)_3]^{2-}$ ($[\mathbf{3}]^{2-}$) in moderate yields. The structures of clusters $[\mathbf{2}]^{2-}$ and $[\mathbf{3}]^{2-}$ have been determined by single-crystal X-ray diffraction as their tetrabutylammonium salts. Cluster **2** forms dimers by interaction of one sulfur atom of the mnt ligand with the anionic binding site of the cluster anion. The structure of **3** reveals the presence of aggregates between the anionic cluster and a Br^- ion. The ESI-MS indicate that these cluster–bromine adducts are also present in solution. Electrochemical studies on complexes **1**–**3** show two irreversible waves associated with reductive cleavage of the disulfido bridges and one or two quasi-reversible oxidation processes for $[Mo_3S_7(ox)_3]^{2-}$ or $[Mo_3S_7(mnt)_3]^{2-}$, respectively. No oxidation waves have been observed for compound **1** or for its thiocyanate derivative $[(n\text{-}Bu)_4N]_2[Mo_3S_7(SCN)_6]$ (**4**) within the acetonitrile solvent window. The optical limiting properties of the complexes **1**–**4** have been measured by the Z-scan technique employing 40 ns pulses at 523 nm. Power limiting was observed for clusters **1**, **2** and **4**, whereas the oxalate derivative **3** was photochemically unstable under our experimental conditions.

1 Introduction

Inorganic cluster compounds are a promising family of non-linear optical (NLO) materials.[1] These compounds offer a great diversity of molecular and electronic structures based on the characteristics of their central core. In particular, sulfur- and selenium-containing clusters with cubane-type structures have been shown to possess strong optical limiting effects.[2,3] We have recently shown that trinuclear and tetranuclear transition metal clusters $[M_3(\mu_3\text{-}Q)(\mu_2\text{-}Q)_3]^{4+}$ and $[M_3Cu(\mu_3\text{-}Q)(\mu_2\text{-}Q)_3]^{5+}$ (M = Mo, W; Q = S, Se) are efficient optical limiters.[4,5] In this work we extend our systematic investigation of the optical properties of cubane-type M_3Q_4 and $M_3M'Q_4$ clusters to complexes containing the $[Mo_3(\mu_3\text{-}S)(\mu_2\text{-}S_2)_3]^{4+}$ unit where the bridging sulfide ligand present in Mo_3S_4 has been replaced by bridging disulfides, $\mu_2\text{-}S_2$.

The chemistry of clusters containing the $[Mo_3(\mu_3\text{-}S)(\mu_2\text{-}S_2)_3]^{4+}$ core has been developed extensively over the past 25 years.[6,7] Derivatives with Mo_3S_7 units are readily accessible by ligand exchange reactions on the $[Mo_3S_7Br_6]^{2-}$ complex, both in the solid state and in solution, due to the lability of the bromine ligands. Examples include various non-reducing ligands such as thiocyanate,[8] dithiocarbamate,[9,10] imidodiphosphinochalcogenido,[11] aniline,[12] catecholate, 2-thiopyridine, 8-hydroxyquinoline[10] and mercapto succinate.[13,14] The Mo_3S_7 cluster unit in all these complexes presents similar structural features with the metal atoms in an equilateral triangular arrangement capped by one apical μ_3-sulfur atom and with the Mo atoms bridged by S_2^{2-} ligands, which results in idealized C_{3v} symmetry for this core. However, a great variety of structures arises due to the electrophilic character[9,15] of the axial sulfur atoms (S_{ax}), those out of the Mo_3 plane, that provides them with the ability to bind: (i) monoanions such as halogens,[10,16,17] ClO_4^-,[9] 7,7,8,8-tetracyanoquinodimethane,[18] (ii) dianions (SO_4^{2-},[9] S^{2-} [19,20]), (iii) the trihapto sulfur atom from another cluster to afford chain structures,[21] or (iv) atoms from the neighboring cluster peripheral ligands[11,22,23] to form dimers.

An appropriate choice of ligands allows the preparation of versatile building blocks for the formation of molecular cluster systems with potential applications as new optical limiting materials or as molecular conductors or magnets. Recently, a series of dithiolene–metal complexes with significant third-order optical nonlinearity have been reported that are promising candidates as active components of optical signal-processing devices.[24,25] A combination of the optical properties of transition metal clusters with those of 1,2-dithiolene ligands can be used to potentially improve the NLO properties of these complexes. In the current work, we present the optical limiting properties of complexes with a Mo_3S_7 core coordinated to a dithiolene group, namely maleonitriledithiolate, and to other ligands with different donor atoms such as oxygen (oxalate), nitrogen (thiocyanate) and halides (bromine). The optical properties are presented together with a complete structural and electrochemical characterization of the reported compounds.

2 Experimental

2.1 Materials and methods

All reactions were performed under a positive pressure of nitrogen. Compounds $(NH_4)_2Mo_3S_{13}$,[26] and $Na_2(S_2C_4N_2)$[27] were prepared according to the literature. ($(n\text{-}Bu)_4N)_2[Mo_3S_7Br_6]$ (**1**)

DOI: 10.1039/b307753e

and $((n\text{-}Bu)_4N)_2[Mo_3S_7(NCS)_6]$ (**4**) were prepared as previously described but using the tetrabutylammonium salt of the trinuclear starting materials instead of tetraethylammonium.[8,28] KSCN, oxalic acid 2-hydrate, Et_3N and the organic solvents were purchased from commercial sources. Elemental analyses was performed on an EA 1108 CHNS microanalytical analyzer at the Universidad de La Laguna. IR spectra were recorded on a Perkin-Elmer System 2000 FT-IR using KBr pellets. Raman spectra were recorded on a Perkin-Elmer System 2000 NIR-FT instrument equipped with a diode-pumped Nd:YAG laser PSU. The position of the sample was manually adjusted, for each case, in order to obtain the maximum intensity for a laser power of 350 mW. Electronic absorption spectra were obtained on a Perkin-Elmer Lambda-19 spectrophotometer. Electrospray mass spectra were recorded with a Micromass Quattro LC instrument, using CH_2Cl_2 as the mobile phase solvent. The samples were added to give a mobile phase of approximate concentration 0.1 mM; nitrogen was employed as a drying and nebulizing gas. Cone voltage was typically varied from 20 to 50 V in order to investigate the effect of higher voltages on the fragmentation pathways of the parent ions. Isotope experimental patterns were compared with theoretical patterns obtained using the MassLynx 3.5 program, Micromass, Manchester, UK, 2000. Cyclic voltammetry experiments were performed with an Echochemie Pgstat 20 electrochemical analyzer. All measurements were carried out at room temperature with a conventional three-electrode configuration consisting of platinum working and auxiliary electrodes and a Ag/AgCl reference electrode containing aqueous 3 M KCl. The solvent used in all experiments was CH_2Cl_2 (HPLC Merck), which was deoxygenated before use. The supporting electrolyte was 0.1 M tetrabutylammonium hexafluorophosphate. $E_{½}$ values were determined as $½(E_a + E_c)$, where E_a and E_c are the anodic and cathodic peak potentials, respectively. All potentials reported were not corrected for the junction potential.

2.2 Preparation of $((n\text{-}Bu)_4N)_2[Mo_3(\mu_3\text{-}S)(\mu_2\text{-}S_2)_3(mnt)_3]$ (2)

An orange solution of $((n\text{-}Bu)_4N)_2[Mo_3S_7Br_6]$ (200 mg 0.136 mmol) in acetonitrile (60 mL) was reacted with $Na_2(S_2C_4N_2)$ (95 mg, 0.51 mmol) under reflux for 12 hours. The resulting dark-brown solution was evaporated under reduced pressure, washed with water, methanol and diethyl ether. Purification by recrystallization from CH_2Cl_2/diethyl ether gave a dark brown solid characterized as **2** (128 mg, 66%). M_w = 1417.2 (Found: C, 37.21; H, 5.12; N, 7.77; S, 29.36. $Mo_3S_{13}C_{44}H_{72}N_8$ requires C, 37.27; H, 5.12; N, 7.91; S, 29.40%). IR KBr cm^{-1}: 2198 (CN, vs), 1143 (S–C, s), 1103 (m), 507 (m), 338 (m). Raman cm^{-1}: 2200 (CN, vs), 1495 (C=C, s), 1495 (C–S, m), 568 (S_{ax}–S_{eq}, s), 380 (m), 340 (Mo–μ_2-S_{eq}, m), 332 (m), 295 (Mo–μ_2-S_{eq}, m), 260 (Mo–μ_3-S, s), 186 (Mo–Mo, m); *m/z* (CH_2Cl_2) 466 $[Mo_3S_7(mnt)_3]^{2-}$, 1175 $[(n\text{-}Bu)_4NMo_3S_7(mnt)_3]^-$ (negative-ion electrospray-MS, 20 V).

2.3 Preparation of $((n\text{-}Bu)_4N)_3[Mo_3(\mu_3\text{-}S)(\mu_2\text{-}S_2)_3(ox)_3]\cdot Br$ (3)

An orange solution of $((n\text{-}Bu)_4N)_2[Mo_3S_7Br_6]$ (150 mg, 0.1 mmol) in acetonitrile (40 mL) was reacted with oxalic acid (H_2ox) (50 mg, 0.39 mmol) in the presence of triethylamine (78 mg, 0.78 mmol) under reflux conditions overnight. The resulting yellow solution, which contains a mixture of the Bu_4N^+ and HEt_3N^+ salts of the desired anionic cluster, was evaporated to dryness under reduced pressure. The solid product was redissolved in water (10 mL) and Bu_4NBr (20 mg, 0.06 mmol) was added to precipitate a yellow solid that was separated by filtration and washed with water. This yellow solid was recrystallized from CH_2Cl_2/diethyl ether to give yellow prismatic crystals characterized as **3** and suitable for X-ray determination (92 mg, 59%). M_w = 1583.6 (Found: C, 43.22; H, 7.35; N, 3.13; S, 14.49 $C_{54}H_{108}N_3O_{12}Mo_3S_7Br$ requires C, 43.13; H 7.24; N, 2.80; S, 14.91%). IR KBr cm^{-1}: 1702 (C=O, vs), 1677 (C=O, vs), 1347 (C–O, s), 786 (m), 528 (m), 352 (m). Raman cm^{-1}: 1710 (C=O, s), 1346 (C–O, s), 531 (S_{ax}–S_{eq}, vs), 368 (s), 342 (Mo–μ_2-S_{eq}, m), 294 (Mo–μ_2-S_{eq}, m), 239, 180 (Mo–Mo, m); *m/z* (CH_2Cl_2) 388 $[Mo_3S_7(ox)_3]^{2-}$, 1341 $\{(n\text{-}Bu_4N)_2[Mo_3S_7(ox)_3]Br\}^-$, 1019 $\{(n\text{-}Bu)_4N[Mo_3S_7(ox)_3]\}^-$ (negative-ion electrospray-MS, 20V).

Table 1 Crystallographic data for $(Bu_4N)_2[Mo_3(\mu_3\text{-}S)(\mu_2\text{-}S_2)_3(mnt)_3]$ (**2**) $(Bu_4N)_3[Mo_3(\mu_3\text{-}S)(\mu_2\text{-}S_2)_3(ox)_3]\cdot Br$ (**3**)

Compound	**2**	**3**
Empirical formula	$C_{44}H_{72}Mo_3N_8S_{13}$	$C_{54}H_{108}BrMo_3N_3O_{12}S_7$
Formula weight	1417.70	1583.58
Crystal system	Monoclinic	Orthorhombic
a/Å	16.019(3)	25.229(9)
b/Å	27.534(5)	23.162(8)
c/Å	15.050(3)	12.495(5)
β/°	98.949(4)	
V/Å^3	6557(2)	7301(5)
Space group (*Z*)	*C*2/*m* (4)	*Pnma* (4)
μ(Mo-Kα)/mm^{-1}	1.014	1.307
Reflections collected	11665	48435
Unique reflections/R_{int}	3519/0.0964	5394/0.0989
$R1^a/wR2^b$ ($I>2\sigma$)	0.0541/0.1437	0.0610/0.1475
$R1^a/wR2^b$ (all data)	0.0964/0.1651	0.0811/0.1591
Max. shift/esd	0.000	0.004
Residual ρ/e Å^{-3}	0.860/−0.523	0.937/−1.097

^{a} $R1 = \Sigma||F_o| - |F_c||/\Sigma F_o$. ^{b} $wR2 = [\Sigma[w(F_o^2 - F_c^2)^2]/\Sigma[w(F_o^2)^2]]^{1/2}$.

2.4 Crystallography

Slow diffusion of CH_3OH into a CH_2Cl_2 solution of **2** or diethyl ether into a CH_2Cl_2 solution of **3** affords crystals suitable for X-ray studies. Single crystals of **2** and **3** were mounted on a glass fiber with silicone grease and transferred to a liquid nitrogen flow at −100 °C. X-Ray diffraction experiments were carried out on a Bruker SMART CCD diffractometer using Mo-Kα radiation (λ = 0.71073 Å). The data were collected with a frame width of 0.3° in Ω and a counting time of 30 s for **2** and 60 s for **3** at a crystal to detector distance of 4 cm. The software SAINT[29] was used for integration of intensity reflections and scaling and SADABS[30] for absorption correction. Final cell parameters were obtained by global refinement of reflections obtained from integration of all frames data. The crystal parameters and basic information relating data collection and structure refinement for compounds **2** and **3** are summarized in Table 1.

The structures were solved by direct methods and refined by the full-matrix method based on F^2 using the SHELXTL software package.[31] The non-hydrogen atoms of the cluster anions in both structures were refined anisotropically. The cluster dianion in **2** and **3** lies on a mirror plane passing through one Mo atom and the maleonitriledithiolate or oxalate ligand attached to it, the capping sulfur and the disulfide ligand bridging the other two Mo atoms. The two tetrabutylammonium cations found per asymmetric unit in **2** are on a two-fold axis. The non-hydrogen atoms within the cation were refined anisotropically; the positions of all hydrogen atoms were generated geometrically, assigned isotropic thermal parameters and allowed to ride on their respective parent carbon atoms. No ordered model could be found for any of the cations in structure **3**. One of the tetrabutylammonium cations in **3** lies on a general position while the nitrogen atom of the other tetrabutylammonium cation lies on a mirror plane. All carbon atoms in the first tetrabutylammonium cation had to be refined isotropically with partial occupancies in two nearby positions. The carbon atoms of the second tetrabutylammonium ion are on general positions and were also refined isotropically with their occupancies fixed at 50%. The hydrogen atoms have not been generated geometrically due to cation disorder.

CCDC reference numbers 211454 and 211455.

See http://www.rsc.org/suppdata/dt/b3/b307753e/ for crystallographic data in CIF or other electronic format.

2.5 Optical limiting studies

Optical measurements of sample solutions in acetonitrile were carried out in 1 mm thick glass cells. Linear optical spectra were obtained on a Cary 4 spectrophotometer over the spectral range 320–900 nm. The system for optical limiting studies employed a Q-switched diode-pumped Nd:YLF laser providing a second harmonic wavelength of 523 nm, pulse length 40 ns, repetition rate *ca*. 20 Hz. The laser pulses were attenuated to approximately 1.5 μJ. The experiments were performed on solutions of concentrations such as to give transmission close to 50%. The power limiting curves were obtained by the open-aperture Z-scan technique,[32] and the data were then converted into transmittance–fluence plots assuming Gaussian character of the beam, the w_0 parameter of the beam being determined from the closed aperture Z-scan results (w_0 was *ca*. 18.5 μm). Note that complex **3** was relatively photochemically unstable and a second Z-scan run performed after the first one always yielded much stronger effects, possibly due to formation of decomposition products. However, a scan performed after moving the sample to a new position, so the laser beam did not irradiate the same spot, yielded the same result as for a pristine sample.

3 Results and discussion

3.1 Synthesis and structure

The lability of the bromine ligands in the $[Mo_3(\mu_3\text{-}S)(\mu_2\text{-}S_2)_3Br_6]^{2-}$ anionic cluster can be conveniently used to prepare a large variety of derivatives. Treatment of $((n\text{-}Bu)_4N)_2[Mo_3(\mu_3\text{-}S)(\mu_2\text{-}S_2)_3Br_6]$ with an excess of disodium maleonitriledithiolate or with oxalic acid in the presence of a base (Et_3N) affords the ligand substitution products with formula $(Bu_4N)_2[Mo_3(\mu_3\text{-}S)(\mu_2\text{-}S_2)_3(mnt)_3]$ (**2**) or $(Bu_4N)_3[Mo_3(\mu_3\text{-}S)(\mu_2\text{-}S_2)_3(ox)_3]\,]\cdot Br$ (**3**), in good yields. It is interesting to point out that the $[Mo_3(\mu_3\text{-}S)(\mu_2\text{-}S_2)_3Br_6]^{2-}$ employed as starting material is prepared by reacting the trinuclear complex $(NH_4)_2[Mo_3S_7(S_2)_3]$ with HBr. However, the reaction of this $[Mo_3S_7(S_2)_3]^{2-}$ cluster with oxalic acid does not afford complex **3**; instead, the cuboidal trimer $[Mo_3S_4(ox)_3(H_2O)_3]^{2-}$ is obtained where ligand substition is accompanied by the reduction of the bridging disulfide to sulfide.[33] A summary of the reactions involved is represented in Scheme 1.

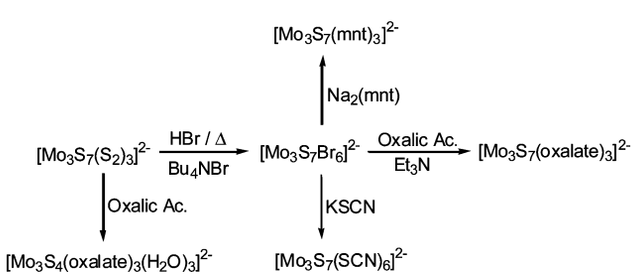

Scheme 1 Reaction scheme for the synthesis of Mo_3S_7 derivatives.

The crystal structures of **2** and **3** share the characteristic features of the Mo_3S_7 core. The cluster anion contains an equilateral Mo_3 triangle capped by a $\mu_3\text{-}S^{2-}$ atom that lies above the Mo_3 plane (1.758 Å for **2** and 1.752 Å for **3**). The mean Mo–Mo distances are 2.7569 and 2.728 Å for **2** and **3**, respectively, consistent with a Mo–Mo single bond. In addition, each side of the triangle is bridged by a $\mu_2\text{-}S_2^{2-}$ group with three sulfur atoms occupying an equatorial position (S_{eq}) essentially in the Mo_3 plane, deviating by less than 0.2 Å and with other axial sulfur atoms (S_{ax}) located out of the trimetallic plane. The maleonitrilodithiolate and oxalate ligands fill the remaining two positions on the seven-coordinated molybdenum atoms and are almost perpendicular to the Mo_3 plane with the distance Mo–Q (Q = O, S) *trans* to μ_3-sulfur atoms being *ca*. 0.05 Å longer than those *cis* disposed.[15] A summary of relevant bond distances for complexes **1**–**3** is presented in Table 2.

Table 2 Selected bond distances (Å) for **1**,[a] **2** and **3**[b]

Compound	$[Mo_3S_7Br_6]^{2-}$	$[Mo_3S_7(mnt)_3]^{2-}$	$[Mo_3S_7(ox)_3]^{2-}$
Mo–Mo	2.747[7]	2.7569[1]	2.728[2]
Mo–μ_3-S	2.340[4]	2.366[1]	2.361[7]
Mo–S_{eq}	2.475[9]	2.503[8]	2.492[1]
Mo–S_{ax}	2.389[11]	2.402[8]	2.410[1]
Mo–L_{trans}[c]	2.64[4]	2.492[2]	2.122[12]
Mo–L_{cis}[d]	2.595[2]	2.438[2]	2.078[4]
S_{eq}–S_{ax}	2.027[2]	2.013[17]	2.059[3]

[a] Ref. 11. [b] Standard deviation for averaged values from one type of bond length are given in square brackets. [c] Mo–L_{trans} distance *trans* to Mo–μ_3-S bond. [d] Mo–L_{cis} distance *cis* to Mo–μ_3-S bond.

In the oxalate complex **3**, the three axial sulfur atoms bind a bromine anion with S ··· Br distances ranging from 2.991 to 3.057 Å. An ORTEP representation of the $[\mathbf{3}]Br^{3-}$ aggregate is depicted in Fig. 1. These intermolecular interactions result in an ordered packing of isolated $[\mathbf{3}]\cdot Br^{3-}$ adducts along the "*b*" direction.

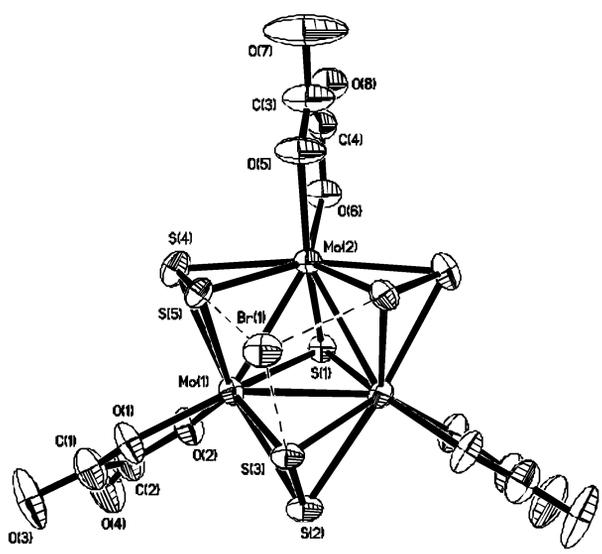

Fig. 1 ORTEP[42] drawing of adduct $\{[Mo_3S_7(C_2O_4)_3]\cdot Br\}^{3-}$ in complex **3** with 50% thermal ellipsoids and atom numbering scheme.

The axial sulfur atoms in the $[Mo_3S_7(mnt)_3]^{2-}$ ($\mathbf{2}^{2-}$) cluster anion interact with the maleonitriledithiolate sulfur atoms of a neighboring cluster with S_{ax}–S_{mnt} intermolecular distances ranging from 3.325 to 3.602 Å and two short contacts between axial sulfur atoms of different clusters, S_{ax}–S_{ax}, of 3.348 Å. These interactions, depicted in Fig. 2, give rise to dimerization of the trimetallic clusters. The sulfur–sulfur bond length within the bridging disulfide is very sensitive towards coordination and we observe an elongation of the S_{ax}–S_{eq} distance of 0.03 Å accompanied by a 0.01 Å lengthening of the Mo–S_{mnt} bond length for those bonds participating in the dimer formation. This lengthening is also reflected in a decrease of the frequency associated with the S_{ax}–S_{eq} stretching vibration (500–570 cm^{-1}). In particular, $[Mo_3S_7(mnt)_3]^{2-}$ presents one Raman frequency at 568 cm^{-1} within the S_{ax}–S_{eq} vibration range and a S_{ax}–S_{eq} bond distance of 2.013 Å. This bond length is slightly longer for $[Mo_3S_7(ox)_3]^{2-}$, $d(S_{ax}\text{–}S_{eq})$ = 2.059 Å and accordingly this complex presents lower values for the S_{ax}–S_{eq} Raman frequencies at 531 cm^{-1}.

A similar phenomenon is observed for the analogous reported dithiolate cluster, namely $(Et_4N)_2[Mo_3S_7(tdt)_3]$ (tdt =

Table 3 Redox potentials of Mo_3S_7 clusters **1** to **4** and $(NH_4)_2[Mo_3S_7(S_2)_3]$ in dichloromethane

Compound	Reduction		Oxidation		Reference
	E_c[b]/V		$E_{½}$ (ΔE[c])/V		
$(Bu_4N)_2[Mo_3S_7Br_6]$[a] (**1**)	−1.15	−1.68	–	–	This work
$(Bu_4N)_2[Mo_3S_7(mnt)_3]$[a] (**2**)	−1.04	−1.71	0.77 (0.071)	1.16 (0.068)	This work
$(Bu_4N)_3[Mo_3S_7(ox)_3]\cdot Br$[a] (**3**)	−1.16	−1.62	0.91 (0.086)	–	This work
$(Bu_4N)_2[Mo_3S_7(SCN)_6]$[a] (**4**)	−0.78	−1.27	–	–	This work
$[(NH_4)_2][Mo_3S_{13}]$	−1.03	−1.28	–		38

[a] $E_{½}$ (ferrocene/ferrocene$^+$) = 0.44 V (ΔE 66 mV). [b] Potentials measured at 100 mV s^{-1}. [c] $\Delta E = |E_a - E_c|$.

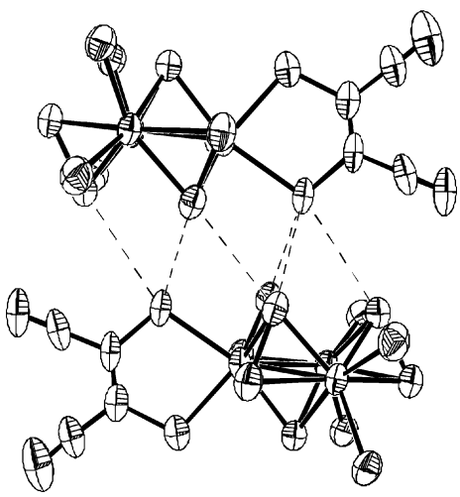

Fig. 2 Dimer formation in structure **2**.

toluene-3,4-dithiolate).[34] The main difference between this structure and that of complex **2** is related to the orientation of the dithiolate ligands as represented in Fig. 3. In the tdt structure, the plane which contains the molybdenum atom and the ligand involved in dimer formation is folded along the S–S hinge by *ca*. 24° while the other two Mo(tdt) planes are only folded by *ca*. 6°. In contrast, no folding is observed for the Mo(mnt) planes in structure **2**.

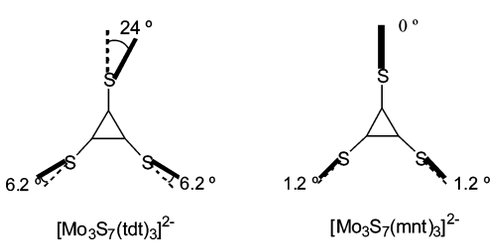

Fig. 3 Orientation of the dithiolate planes with respect to the Mo_3 plane in $[Mo_3S_7(tdt)_3]^{2-}$ and $[Mo_3S_7(mnt)_3]^{2-}$ cluster complexes.[34]

There is a consensus opinion that the electrospray ionization source in mass spectrometry experiments (MS-ES) simply transfers to the gas phase pre-formed ions in solution.[35] In order to investigate the presence in solution of the $[Mo_3S_7(mnt)_3]_2^{4-}$ dimers found in **2** and the $\{[Mo_3S_7(ox)_3]Br\}^{3-}$ aggregate encountered in **3** we carried out MS-ES experiments on these systems. Dichloromethane solutions of **2** give signals corresponding to the $[Mo_3S_7(mnt)_3]^{2-}$ double charged ion and also to the $\{(Bu_4N)[Mo_3S_7(mnt)_3]\}^-$ aggregate but no signal due to the quadruply charged dimer could be observed. However, dichloromethane solutions of **3** show in addition to the peaks found for **2**, one peak at 1341 mass units that can be assigned to the $\{(Bu_4N)_2[Mo_3S_7(ox)_3]Br\}^-$ adduct based on the excellent agreement between the experimental and calculated isotopic peak distribution. Theoretical studies of the nature of this interaction suggest that it is mainly electrostatic in spite of the anionic nature of its constituents.[9] Fragmentations at high cone-voltage show the loss of terminal monodentate ligands in complexes **1** and **4** while peaks due to the loss of the sulfur atoms from the disulfido bridges are observed for compounds **2** and **3** with bidentate terminal ligands. In a previously reported FAB mass spectrometry study, evidence was provided for a similar fragmentation scheme to that observed for **2** and **3**.[19,36,37]

3.2 Redox properties

The redox properties of compounds **1**–**4** in CH_2Cl_2 solution have been investigated by cyclic voltammetry and the results compared with those previously reported for other Mo_3S_7 clusters. A summary of electrochemical data for these complexes is presented in Table 3.

Electrochemical investigations on Mo_3S_7 clusters are limited to a few complexes, in contrast with the large variety of ligands that have been coordinated to this cluster unit.[23,38] All complexes reported undergo two reduction processes whose potentials show a negligible dependence on the nature of the ligand or on the total charge of the compound. Such processes have been attributed to the reductive cleavage of the disulfide bridges and this hypothesis has been confirmed by molecular orbital calculations. The LUMO orbital for these systems is mainly located on the bridging S_2^{2-} ligand and has antibonding p–π*/σ* character.[9,39] These observations agree in general terms with our experimental results except for the reduction potentials found for **4**. The first reduction potential measured for the thiocyanate derivative **4** is anodically shifted by *ca*. 0.45 V compared with the values reported for other complexes including **1**–**3**. This result suggests that in some cases the ligand influences the reduction behaviour of Mo_3S_7 clusters.

No oxidation processes have been reported up to now for Mo_3S_7 clusters, a circumstance that has been attributed to the nature of the HOMO orbital calculated for the $Mo_3S_{13}^{2-}$ complex. This orbital is mainly formed by weakly interacting p* orbitals from the terminal S_2^{2-} ligand. Based on this one would expect that changes in the terminal ligands could lead to changes in the oxidation behaviour. This is what we observe for complexes **2** and **3** which show one and two quasi-reversible waves, respectively, suggesting a contribution from the ligand to the HOMO orbital. The dithiolene complex **2** is easier to oxidize than the oxalate derivative **3**.

3.3 Optical limiting properties

The linear and nonlinear optical properties of **1**–**4** have been assessed, the results from which are collected in Table 4. Linear optical spectra of all complexes possess intense bands at high energy. The S-donor 1,2-ethylenedithiolato complex **2** is relatively strongly absorbing at lower energy, in contrast to the Br, O-donor and N-donor ligated **1**, **3** and **4**.

Relevant data for optical limiting merit are collected in Table 4; all four clusters absorb at the measurement wavelength of 523 nm, **1**, **3** and **4** weakly and **2** somewhat more strongly. Optical limiting in the current clusters has been assessed using the Z-scan technique. Closed aperture Z-scan is usually used to

Table 4 Linear optical and optical limiting data for clusters **1**–**4**

Cluster	ε_{523}/dm^3 mol^{-1} cm^{-1}	$F_{15\%}$/J cm^{-2} [a]	Cross section/10^{-18} cm^2	
			Ground state, σ_0	Excited state, σ_{eff}
$(NBu_4)_2[Mo_3S_7Br_6]$ (**1**)	300	0.15	1.1	2.3
$(NBu_4)_2[Mo_3S_7(mnt)_3]$ (**2**)	4200	0.2	16	18
$(NBu_4)_3[Mo_3S_7(ox)_3]\cdot Br$ (**3**)	90	0.3	0.35	3.0
$(NBu_4)_2[Mo_3S_7(NCS)_6]$ (**4**)	372	0.2	1.4	11

[a] $F_{15\%}$ is defined as the incident fluence needed to reduce the transmittance through the sample by 15%.

derive the nonlinear refractive index intensity coefficient n_2 by examining self-focusing or self-defocusing phenomena.[40] To determine the nonlinear absorption properties, the total transmission through a sample can be monitored by employing open-aperture Z-scan. We have previously discussed the utility and shortcomings of this experimental procedure to evaluate optical limiting,[4] the major problem being that with nanosecond, non-time-resolved measurements the power-limiting mechanism remains obscure.

Open- and closed-aperture Z-scan plots for a representative compound (**2**) are displayed in Fig. 4. Our two earlier reports[4,5] found power limiting at fluences of the order of 100 mJ cm^{-2}. In the present study, power limiting was observed in **1**, **2** and **4** (compound **3** was photochemically unstable under our experimental conditions, but reproducible results could be obtained from the initial Z-scan traces of previously non-irradiated material). We reiterate here that, with about 40 ns pulses from the laser, the power limiting is likely to involve several different contributions, the thermal contributions likely being important.

Transmission *vs*. fluence plots were generated for all clusters, a representative example (that of **4**) being shown in Fig. 5. As before,[4] we have utilized a threshold limiting fluence $F_{15\%}$ (defined as the incident fluence needed to reduce the transmittance through the sample by 15%) to assess the relative optical limiting merit of these clusters, the results being tabulated in Table 4. Data from **1**, **2** and **4** fall within a narrow range (and indeed a narrower range than we noted previously for cluster core metal variation in a related series[4]), suggesting that the inherent ligand replacement across the present series is not a critical factor affecting threshold limiting fluence; however, a full quantitative comparison is not possible given the widely differing absorptivities of the solutions at the measurement wavelength.

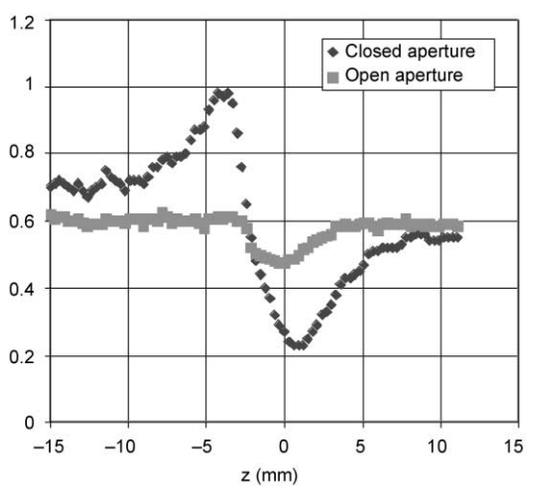

Fig. 4 Open and closed aperture Z-scans for solutions of complex **2**.

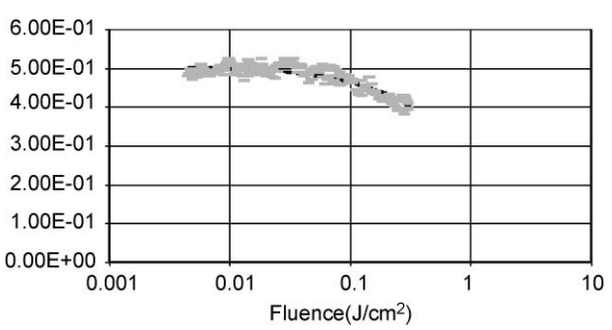

Fig. 5 Power limiting plot for **4** together with theoretical fit.

To provide quantitative comparisons between the different compounds investigated here, we have analyzed the power limiting in the framework of formulae given in reference 41. The transmittance of the cell is taken as:

$$T = (1-R)^2 \frac{\exp(-\alpha_0 L)}{q} \ln(1+q)$$

where

$$q = (1 - R)[1 - \exp(-\alpha_0 L)\delta_{eff} F_0/2F_s$$

and R is the reflection coefficient, α_0 is the low power absorption coefficient, F is the fluence and F_s is the saturation fluence defined as

$$F_s = \frac{\hbar\omega}{\sigma_0}$$

and

$$\delta_{eff} = \frac{\sigma_{eff} - \sigma_0}{\sigma_0}$$

where σ_0 is the ground-state cross-section.

The effective excited state cross section σ_{eff} should be treated as only a measure of the power limiting ability of the substance under given experimental conditions: it may contain contributions from several different excited states with different properties (*e.g.* from both a singlet and a triplet state). Values of excited-state cross-section σ_{eff} for **1**–**4** are given in Table 4; data for **1**, **2** and **4** are larger than those of the corresponding ground-state cross-section σ_0, *i.e.* **1**, **2** and **4** are efficient optical limiters.

Acknowledgements

This work has been supported by the "Ministerio de Ciencia y Tecnologia" (research project BQ2002-00313), Generalitat Valenciana (research project CTIDIB/2002/330) and Fundació Caixa Castelló-UJI (research project P1.1B2001–07). Thanks are also extended to the Servei Central d'Instrumentació Científica for providing us with mass spectrometry, nuclear resonance and X-ray facilities. M. G. H. thanks the Australian Research Council for a Senior Research Fellowship. A. J. U. is and N. T. L. was the recipient of an Australian Postgraduate Award.

References

1 S. Shi, in *Optoelectronic Properties of Inorganic Compounds*, ed. D. M. Roundhill and J. P. Fackler, Jr., Plenum, New York, 1999.
2 Q.-F. Zhang, M.-T. Bao, M.-C. Hong, R. Cao, Y.-L. Song and X.-Q. Xin, *J. Chem. Soc., Dalton Trans.*, 2000, 605.
3 Q.-F. Zhang, Y.-N. Xiong, T.-S. Lai, W. Ji and X.-Q. Xin, *J. Phys. Chem. B*, 2000, **104**, 3446.
4 M. Feliz, J. M. Garriga, R. Llusar, S. Uriel, M. G. Humphrey, N. T. Lucas, M. Samoc and B. Luther-Davies, *Inorg. Chem.*, 2001, **40**, 6132.
5 M. Feliz, R. Llusar, S. Uriel, C. Vicent, M. G. Humphrey, N. T. Lucas, M. Samoc and B. Luther-Davies, *Inorg. Chim. Acta*, 2003, **349**, 69.
6 T. Shibahara, *Coord. Chem. Rev.*, 1993, **123**, 105.
7 A. Müller and E. Krahn, *Angew. Chem., Int. Ed. Engl.*, 1995, **34**, 1071.
8 V. P. Fedin, M. N. Sokolov, V. Y. Fedorov, D. S. Yufit and Y. T. Struchkov, *Inorg. Chim. Acta*, 1991, **179**, 35.
9 M. J. Mayor-López, J. Weber, K. Hegetschweiler, M. D. Meienberger, F. Joho, S. Leoni, R. Nesper, G. J. Reiss, W. Frank, B. A. Kolesov, V. P. Fedin and V. E. Fedorov, *Inorg. Chem.*, 1998, **37**, 2633.
10 H. Zimmermann, K. Hegetschweiler, T. Keller, V. Gramlich, H. Schmalle, W. Petter and W. Schneider, *Inorg. Chem.*, 1991, **30**, 4336.
11 V. Bereau, C. G. Pernin and J. A. Ibers, *Inorg. Chem.*, 2000, **39**, 854.
12 V. P. Fedin, Y. Mironov, V. Virovets, N. V. Podberezskaya and V. Y. Fedorov, *Polyhedron*, 1992, **11**, 2083.
13 K. Hegetschweiler, T. Keller, H. Zimmermann, W. Schneider, H. Schmalle and E. Dubler, *Inorg. Chim. Acta*, 1990, **169**, 235.
14 E. A. Il'inchik, V. Volkov, O. V. Volkov, I. P. Asanov and B. A. Kolesov, *Russ. J. Coord. Chem.*, 2000, **26**, 185.
15 A. V. Virovets and N. V. Podberezskaya, *J. Struct. Chem.*, 1993, **1993**, 305.
16 G. Borgs, H. Keck, W. Kuchen, D. Mootz, R. Wiskeman and H. Wunderlich, *Z. Naturforsch., B*, 1991, **46**, 1525.
17 J. Chen, S. F. Lu, Z. X. Huang, R. M. Yu and Q. J. Wu, *Chem. Eur. J.*, 2001, **7**, 2002.
18 V. P. Fedin, M. N. Sokolov, A. V. Virovets, N. V. Podberezskaya and V. Y. Fedorov, *Inorg. Chim. Acta*, 1994, **194**, 195.
19 M. D. Meienberger, K. Hegetschweiler, V. Ruegger and V. Gramlich, *Inorg. Chim. Acta*, 1993, **213**, 157.
20 H. Zhu, Q. Liu, C. Chen and Y. Deng, *Chinese J. Struct. Chem. (Jiegou Huaxue)*, 1998, **17**, 142.
21 A. Müller, V. Wittneben, E. Krickemeyer, H. Bögge and M. Lemke, *Z. Anorg. Allg. Chem.*, 1991, **605**, 175.
22 C. C. Raymond, P. K. Dorhout and S. M. Miller, *Inorg. Chem.*, 1994, **33**, 2703.
23 K. Hegetschweiler, T. Keller, M. Bäumle, G. Rihs and W. Schneider, *Inorg. Chem.*, 1991, **30**, 4342.
24 J. L. Zuo, T. M. Yao, F. You, X. Z. You, H. K. Fun and B. C. Yip, *J. Mater. Chem.*, 1996, **6**, 1633.
25 J. Dai, G. Q. Bian, X. Wang, Q. F. Xu, M. Y. Zhou, M. Munakata, M. Maekawa, M. H. Tong, Z. R. Sun and H. P. Zeng, *J. Am. Chem. Soc.*, 2000, **122**, 11007.
26 A. Müller, S. Sarkar, R. G. Bhattacharyya, S. Pohl and M. Dartmann, *Angew. Chem., Int. Ed. Engl.*, 1978, **17**, 535.
27 A. Davison and R. H. Holm, *Inorg. Synth.*, 1967, **10**, 8.
28 V. P. Fedin, M. N. Sokolov, Y. V. Mironov, B. A. Kolesov, S. V. Tkachev and V. Y. Fedorov, *Inorg. Chim. Acta*, 1990, **167**, 39.
29 SAINT, Bruker Analytical X-Ray Systems, Madison, WI, 1996.
30 G. M. Sheldrich, SADABS empirical absorption program, University of Göttingen, Germany, 1996.
31 G. M. Sheldrich, SHELXTL, Bruker Analytical X-Ray Systems, Madison, WI, 1997.
32 M. Sheik-Bahae, A. A. Said, T. Wei, D. J. Hagan and E. W. van Stryland, *IEEE J. Quantum Electron.*, 1990, **26**, 760.
33 F. A. Cotton, R. Llusar, D. O. Marler and W. Schwotzer, *Inorg. Chim. Acta*, 1985, **102**, L25.
34 S. F. Lu, Q. J. Wu, H. B. Chen, R. M. Yu and J. Q. Hung, *Chinese J. Struct. Chem. (Jiegou Huaxue)*, 1994, **13**, 389.
35 W. Henderson, B. K. Nicholson and L. J. McCaffrey, *Polyhedron*, 1998, **17**, 4291.
36 K. Hegetschweiler, T. Keller, W. Amrein and W. Schneider, *Inorg. Chem.*, 1991, **30**, 873.
37 K. Hegetschweiler, P. Caravatti, V. Fedin and M. N. Sokolov, *Helv. Chim. Acta*, 1992, **75**, 1659.
38 A. Müller, R. Jostes, W. Jaegermann and R. G. Bhattacharyya, *Inorg. Chim. Acta*, 1980, **41**, 259.
39 A. Müller, R. Jostes and F. A. Cotton, *Angew. Chem., Int. Ed. Engl.*, 1980, **19**, 875.
40 I. R. Whittall, A. M. McDonagh, M. G. Humphrey and M. Samoc, *Adv. Organomet. Chem.*, ed. F. G. A. Stone, R. West and A. F. Hill, San Diego, 1999, vol. 43, p. 349.
41 R. L. Sutherland, *Handbook of Nonlinear Optics*, Marcel Dekker, New York, 1996.
42 M. N. Burnett and C. K. Johnson, ORTEP-III, Oak Ridge Thermal Ellipsoid Plot Program for Crystal Structure Illustrations, Report ORNL-6895, Oak Ridge National Laboratory, Oak Ridge, TN, USA, 1996.